The DOI for this manuscript is doi: 10.1175/2010JHM1224.1

A new global 0.5° gridded dataset (1901–2006) of a multiscalar drought index: comparison with current drought index datasets based on the Palmer Drought Severity Index

Vicente-Serrano, S.M.[1], Beguería, S.[2], López-Moreno, J.I.[1], Angulo, M.[2], El Kenawy, A.[1]

1) Instituto Pirenaico de Ecología, CSIC (Spanish National Research Council), Campus de Aula Dei, P.O. Box 202, Zaragoza 50080, Spain.
2) Estación Experimental de Aula Dei CSIC (Spanish National Research Council), Zaragoza, Spain.
svicen@ipe.csic.es

Abstract: A monthly global dataset of a multiscalar drought index is presented and compared in terms of spatial and temporal variability with the existing continental and global drought datasets based on the Palmer drought severity index (PDSI). The presented dataset is based on the standardized precipitation evapotranspiration index (SPEI). The index was obtained using the CRU TS3.0 dataset at a spatial resolution of 0.5°. The advantages of the new dataset are that; i) it improves the spatial resolution of the unique global drought dataset at a global scale; ii) it is spatially and temporally comparable to other datasets, given the probabilistic nature of the SPEI, and, in particular; iii) it enables identification of various drought types, given the multiscalar character of the SPEI. The dataset is freely available on the web page of the Spanish National Research Council (CSIC) in three different formats (NetCDF, binary raster, and plain text).

Keywords: drought; drought index, standardized precipitation evapotranspiration index, SPEI, Palmer drought severity index, PDSI, climate data, global dataset, standardized precipitation index, SPI.

1. Introduction

One of the priorities of the climate sciences is the development of reliable datasets to analyze climate processes at spatial scales ranging from continental to global. Most effort has been devoted to the development of global gridded datasets of various climate variables including temperature, precipitation, and pressure. Access to most of the datasets is through the Climate Explorer (http://climexp.knmi.nl) of the Dutch Royal Meteorological Institute (Koninklijk Nederlands Meteorologisch Instituut).

Notwithstanding the usefulness of these datasets, there is a need for datasets of basic climate parameters and synthetic information about moisture and dryness conditions; these are highly valued by environmental, hydrological, and global change researchers, and are indispensable for determining the possible impacts of climate variability and change. The best approach to obtaining a measure of relative wetness or dryness is the calculation of drought indices (Heim, 2002; Keyantash and Dracup, 2002).

Among various indices for drought detection, the Palmer drought severity index (PDSI; Palmer, 1965) is one of the most widely used; the calculation procedure for this index has been described in several studies (*e.g.,* Karl, 1983, 1986; Alley, 1984). This is a climatic water balance index that considers precipitation and evapotranspiration anomalies, and soil water-holding capacity. Many of the PDSI deficiencies were resolved by development of the self-calibrated PDSI (sc-PDSI) (Wells et al., 2004), which is spatially comparable and reports extreme wet and dry events at frequencies expected for rare conditions. All currently available gridded drought datasets at continental and global scales are based on either the PDSI or the sc-PDSI (Dai et al., 2004; Van del Schrier et al., 2006a and 2006b).

The PDSI has a fixed temporal scale, which does not allow different drought types (*e.g.,* hydrological, meteorological, agricultural, and socioeconomic) to be distinguished. This is an important shortcoming because drought is a multiscalar phenomenon (McKee et al., 1993) because drought is a phenomenon which may occur simultaneously across multiple temporal scales (for example, a short period of particular dryness embedded within a long-term drought). Therefore, multi- refers to numerous, temporal periods which may or may not overlap. The response of various hydrological systems (including soil moisture, ground water, snowpack, river discharge, and reservoir storage) to precipitation can vary markedly as a function of time (Changnon and Easterling, 1989; Elfatih et al., 1999; Pandey and Ramasastri, 1999). The need for a drought index that considers the multiscalar nature of droughts explains the wide acceptance of the SPI, which was developed by McKee et al. (1993). This index can be calculated at varying time scales to monitor droughts with respect to different usable water resources (e.g., Szalai et al., 2000; Ji and Peters, 2003; Vicente-Serrano and López-Moreno, 2005; Khan et al., 2008; Lorenzo-Lacruz et al., 2010).

However, the SPI has the important shortcoming that it is based only on precipitation data, and does not consider other critical variables such as evapotranspiration, which can have a marked influence on drought conditions. Abramopoulos et al. (1988) used a general circulation model experiment to show that evaporation and transpiration can consume up to 80% of rainfall. In addition, the authors found that the fraction of drying caused to temperature anomalies is as high as that attributable to rainfall shortage. Therefore, it is preferable to use drought indices that include temperature data in formulation of datasets such as the PDSI. However, the PDSI lacks the multiscalar character essential for determining the impact of droughts on different hydrological systems, crops, and natural vegetation, and for differentiating among various drought types. For this reason, Vicente-Serrano et al. (2010) formulated a new drought index (the standardized precipitation evapotranspiration index; SPEI) based on precipitation and potential evapotranspiration (PET). The SPEI combines the sensitivity of the PDSI to changes in evaporation demand (caused by temperature fluctuations and trends) with the multitemporal nature of the SPI.

Here we present a new global drought dataset based on the SPEI, which covers time scales from 1-48 months at a spatial resolution of 0.5°, and provides temporal coverage for the period 1901-2006. This dataset represents an improvement in the spatial resolution and operative capability of previous gridded drought datasets based on the PDSI, and enables identification of various drought types.

2. Methodology

To calculate the SPEI we used the CRU TS3 dataset (available at http://badc.nerc.ac.uk/browse/badc/cru/data). This is the most complete and updated dataset of gridded precipitation and temperature at the global scale, has a spatial resolution of 0.5°, and covers the period 1901–2006.

The SPEI is based on the climatic water balance i.e. the difference between precipitation and PET:

$$D = P - PET, \qquad \text{(eq. 1)}$$

where P is the monthly precipitation (mm) and PET (mm) is calculated according to the method of Thornthwaite (1948), which only requires data on mean monthly temperature and the geographical location of the region of interest.

The calculated D values were aggregated at various time scales:

$$D_n^k = \sum_{i=0}^{k-1} \left(P_{n-i} - PET_{n-i}\right), \; n \geq k \qquad \text{(eq. 2)}$$

where k (months) is the timescale of the aggregation and n is the calculation number. The D values are undefined for $k > n$.

A log-logistic probability distribution function was then fitted to the data series of D, as it adapts very well to all time scales. The complete calculation procedure for the SPEI can be found in Vicente-Serrano et al. (2010).

We tested the goodness of fit between the global monthly series of D^k at time scales from 1–48 months, and the log-logistic distribution. This was checked using the Kolmogorov-Smirnov (KS) test at a critical level α = 0.05. The KS test is based on the KS distance statistic, which quantifies the maximum vertical distance between the empirical cumulative distribution function (ECDF) of the sample (the 1901–2006 series of D^k) and the cumulative distribution function (CDF) of the reference distribution. In this case the ECDF was calculated using the plotting position formula proposed by Hosking (1990) for highly skewed data.

We compared the multiscalar SPEI dataset with the available PDSI-based datasets at global and continental scales, and assessed its capabilities. For this purpose we used the global PDSI at 2.5°, developed by the University Corporation for Atmospheric Research (UCAR, Dai et al., 2004). We also used the European and North American 0.5° sc-PDSI grids, developed by the Climate Research Unit (CRU) of the University of East Anglia (van der Schrier, 2006a, 2006b). Both datasets were obtained using precipitation and temperature data from the CRU TS 2.1 datasets (Mitchell and Jones, 2005). The datasets span the period 1901–2002 and the regions 20–50°N and 130–60°W for North America, and 35–70°N and 10°W–60°E for Europe.

3. Results

3.1. Goodness of fit of the global SPEI dataset

Figure 1 shows results from application of the KS test to the global SPEI dataset for January and July, at time scales of 1, 4, and 12 months. This enabled the log-logistic distribution for most parts of the world to be accepted, because the null hypothesis (that the data came from a log-logistic distribution) was rejected for only very few areas. In most regions the P value for the KS distance statistic was well above 0.45, indicating that the log-logistic distribution was highly suitable for fitting the D^k series. Only for the shortest time scales and for regions of poor data availability (such as northern Siberia, Greenland, and the Himalayas) did the D^k series fail to match the log-logistic distribution. For most time scales and months the log-logistic distribution fitted the D^k series very well across most of the world. The global percentage oscillates between 85% and 97% as a function of the time scale and the month. Therefore, the selected log-logistic distribution was considered highly appropriate for calculation of the SPEI in most regions, independent of the month and time scale of analysis.

3.2. Comparison with other drought gridded datasets

Figure 2 shows the spatial distribution of the UCAR PDSI and the SPEI at selected time scales for August 1936, a month in which major drought conditions occurred in some regions of North America and Russia. Comparison of these datasets showed the greater spatial resolution of the SPEI dataset, which facilitates local and regional analysis. The SPEI dataset shows some similarity in the intensity and spatial distribution of drought conditions worldwide. Nevertheless, large differences can be extracted as a function of the time scale of analysis. For example, in South Africa and Namibia the PDSI showed moderate drought conditions for the majority of the region, but the SPEI clearly showed that drought conditions were particularly severe at short time scales (3 months), whereas at the longest time scales such episodes were not recognized. A similar pattern was evident for drought conditions in Australia, which were mainly characterized by short time scales. The PDSI seemed to respond differently to varying time scales of drought in different regions of the world. For example, in northwest Canada and Alaska the humid conditions recorded in August 1936 by the PDSI were also recorded by the SPEI at the longest time scales (24-36 months). In other regions, including Scandinavia, the normal conditions (values close to 0) recorded by the PDSI were identified by the SPEI at short time scales; at longer time scales (12-24 months) the SPEI showed very humid conditions in these areas. The opposite pattern was found for the humid conditions in August 1936 in southwest Europe, where the strongest agreement between the PDSI and the SPEI occurred at time scales of 9-12 months.

Figure 3 shows a similar comparison involving the CRU sc-PDSI dataset for Europe for November 1949. The drought pattern from the sc-PDSI showed very few similarities with the SPEI at the 3-month time scale, where the sc-PDSI indicated that the most extreme drought conditions were in the Baltic countries and eastern Germany. France, the Iberian Peninsula, and large areas of the Balkans showed humid conditions. At the 6-month time scale the most severe drought conditions were recorded in Germany, France, and Switzerland, with very humid conditions being recorded in most of the Balkans. Thus, the very humid conditions recorded in Italy and the Balkans at time scales of 3-9 months were not identified using the sc-PDSI.

In summary, these two examples show that the existing drought datasets, based on the PDSI and the sc-PDSI, are too rigid to identify droughts of varying temporal scales (short-, medium-, and long-term). In addition, the relative conditions of dryness and humidity indicated by the PDSI and the sc-PDSI are sometimes erroneous, as they may result from very dry conditions over short time scales and very humid conditions over long time scales (and vice versa). However, the SPEI enabled detection of droughts at numerous time scales.

Figure 4 shows the average correlation and standard deviation between the CRU sc-PDSI and the SPEI at several time scales for Europe and North America, and also between the global UCAR PDSI and the SPEI. Correlations were calculated for each time series of 0.5° (for Europe and North America; sc-PDSI) and 2.5° (globally, aggregating the SPEI pixels of 0.5° to 2.5°). Although the correlations differed in magnitude between the global, European, and North American datasets (the highest correlations were found for the sc-PDSI in Europe, and the lowest for the global PDSI), the three datasets showed maximum correlations with the SPEI at time scales of 6-18 months, with a maximum in all cases at the time scale of 12 months.

These differences are clearly very important if relationships between PDSI-based indices and the different time scales of the SPEI are analyzed spatially. Figure 5 shows the spatial distribution of correlations between the UCAR PDSI and the SPEI at different time scales. At a time scale of 3 months, only in eastern USA and Australia were large areas recorded with correlations greater than 0.6; in most other regions the correlation between the PDSI and the 3-month SPEI was very low. For the SPEI, the correlation increased in magnitude and spatial extent at time scales of 6-12 months, but, in some regions (Canada, Central America, central Africa, and parts of Asia), correlations between the SPEI and the PDSI were very low, independent of the time scale analyzed. At time scales of 18-48 months the relationship between the PDSI and the SPEI decreased. The maps show that, although at time scales of 9-18 months correlations were in general very high over large regions of the world ($R > 0.8$), in some regions the PDSI could represent drought conditions at a different time scale. In Australia, for example, the PDSI tended to be reflecting shorter time scales than shown for eastern Europe and the eastern USA. Thus, very great spatial variability was evident in maps showing the time scales at which the correlation between the SPEI and the PDSI was highest.

Comparison of the CRU sc-PDSI with the SPEI also showed differences in the spatial patterns and magnitudes of correlations, and the time scale of the SPEI showing the highest correlation with the sc-PDSI. Figure 6 shows the spatial distribution of correlations between the sc-PDSI and the SPEI at different time scales in Europe. The pattern shows weak correlations at the 3-month time scale (although there were some exceptions), and an increase in the magnitude and surface extent of correlations at time scales of 6-12 months. The high correlations were maintained for the 18- and 24-month SPEI intervals, but decreased thereafter. Most of the European continent showed correlations higher than 0.6 between the sc-PDSI and the SPEI. Nevertheless, whereas in North America maximum correlations were recorded at time scales of 9-12 months (not shown), in Europe the maximum correlations were found at time scales of 12-18 months. However, in some areas of the Mediterranean region, the highest correlations were recorded at time scales of 3-6 months.

4. Discussion and Conclusions

We have described a new global gridded dataset of a multiscalar drought index; the standardized precipitation evapotranspiration index (SPEI), which considers the joint effects of temperature and precipitation on droughts. The dataset has some advantages regarding existing global and continental drought datasets. SPEI improves the spatial resolution (0.5º) of the unique global dataset, based on the Palmer drought severity index (UCAR-PDSI, 2.5º). Moreover, the global gridded SPEI incorporates recent high-resolution gridded precipitation and temperature data (CRU TS3.0). Nevertheless, the main advantage of the new dataset lies in its multiscalar character, which allows discrimination between different types of drought.

With very few exceptions, for most regions worldwide a good fit was found between the log-logistic distribution and the precipitation–evapotranspiration D^k series, independent of the time scale k and the month of the year. This guarantees the robustness of SPEI calculations based on such probability distributions.

The SPEI was largely comparable to the PDSI, as both indices consider water inputs by precipitation and water outputs by evapotranspiration. However, comparison between the SPEI, the global PDSI, and the continental (North America and Europe) sc-PDSI datasets, showed that the PDSI and the sc-PDSI both have a rigid time scale. When a drought condition is recorded with the SPEI on a particular time scale, it is possible to establish that the drought was caused by cumulative precipitation deficit and/or excessive evapotranspiration (relative to average conditions) during the previous time scale period.

We showed that both the PDSI and the sc-PDSI were generally correlated with the SPEI at time scales of 12-18 months, and, thus, the PDSI can be considered as an index representing water deficits at these time scales. Then we conclude that the PDSI is not a reliable index for identifying either the shortest or the longest time scale droughts, which can have greater impacts on ecological and hydrological systems than droughts at the intermediate time scales represented by the PDSI. This suggests that PDSI has a limited capacity to describe the impact of droughts on a range of natural systems. With respect to hydrological systems, Vicente-Serrano and López-Moreno (2005) found that the variability of river discharge in a mountainous area of northern Spain was highly correlated with drought-as described by the SPI- at very short time scales (2–3 months), whereas reservoir storages were more related to time scales of 8-12 months. Lorenzo-Lacruz et al. (2009) found that reserves in high-capacity reservoirs of central Spain were closely related to drought indices at long time scales (36-48 months). Moreover, river discharges in the headwaters of the basins were referable to time scales of 4-8 months, whereas runoff variability in the middle and lower reaches were better explained at longer time scales (up to 12 months), with particular reference to variability of flow (López-Moreno et al., 2009). In Australia, Khan et al. (2008) analyzed fluctuations in the water table level in different basins, and related these to varying time scales of droughts. The cited authors found great spatial diversity in responses. Thus, in some basins, the clearest response occurred at the 6-month time scale, but in others the highest correlation was found at time scales of 12-24 months.

Cultivation and natural vegetation cover also vary markedly in response to drought, at different time scales. Vicente-Serrano (2007) showed that the vegetation activity in steppe areas and cereal drylands of semiarid regions of the Iberian Peninsula was closely related to short time scales (3-6 months), whereas forests responded more to longer time scales. Many studies have described variable responses of usable water sources, vegetation, and crops to droughts over various time scales (*e.g.,* Szalai et al., 2000; Ji and Peters, 2003; Vicente-Serrano et al., 2006; Patel et al., 2007; Hoffman et al., 2009; Strenberg et al., 2009). Therefore, only hydrological and economic systems that respond to water deficits at time scales of 9-18 months can be monitored using the PDSI or the sc-PDSI. For other systems not sensitive at these time scales, the PDSI is not useful for analysis of drought conditions or impacts.

We also found that the time scale represented by the PDSI is not fixed at global or continental scales. The strongest correlation between the PDSI and the SPEI at different time scales varied noticeably among regions. This implies that the manner in which the PDSI represents water deficits at different time scales depends on the world region under consideration. Although this issue has not been identified as a limitation of the PDSI in previous studies, this is nonetheless an important drawback that makes the spatial comparability of droughts difficult using this index. This pattern has also been observed with use of the sc-PDSI in the USA and Europe. Thus, in some regions, the PDSI provides information on short-term droughts, whereas in most areas the PDSI is a medium-term (9-18 months) or long-term drought index (*e.g.,* in central USA, west Africa, and eastern Europe).

In summary, because of the great complexity of drought impacts on different sectors and natural systems, it is desirable to use an index that can be calculated over different time scales, and the SPEI fulfils this criterion. The strict probabilistic nature of this index makes it perfectly comparable across time and space; the index provides objective information on climatic drought conditions, as the index is not influenced by external variables, relying only on climate data. The index incorporates the role of water inputs (precipitation) and outputs (evapotranspiration), is able to identify climate change processes related to alterations in precipitation and/or temperature, and can be used to assess the possible influences of warming processes on droughts. The global gridded SPEI dataset described here (spatial resolution 0.5°; period 1901–2006, time scale 1-48 months) is freely available in plain text, binary raster, and NetCDF formats in the Web repository of the Spanish Scientific Council Agency (CSIC), at http://hdl.handle.net/10261/22449.

Acknowledgements

This work has been supported by the research projects CGL2008-01189/BTE and CGL2006-11619/HID financed by the Spanish Commission of Science and Technology and FEDER, EUROGEOSS (FP7-ENV-2008-1-226487) and ACQWA (FP7-ENV-2007-1- 212250) financed by the VII Framework Programme of the European Commission, "Las sequías climáticas en la cuenca del Ebro y su respuesta hidrológica" and "La nieve en el Pirineo aragonés: Distribución espacial y su respuesta a las condiciones climática" Financed by "Obra Social La Caixa" and the Aragón Government.

References

Abramopoulos, F., Rosenzweig, C. and Choudhury B., (1988): Improved ground hydrology calculations for global climate models (GCMs): Soil water movement and evapotranspiration. *Journal of Climate* 1: 921–941.

Alley, W.M., (1984): The Palmer drought severity index: limitations and applications. *Journal of Applied Meteorology,* 23: 1100-1109.

Changnon, S.A. and Easterling, W.E., (1989): Measuring drought impacts: the Illinois case. *Water Resources Bulletin.* 25: 27-42.

Dai, A., Trenberth, K.E., and Qian, T., (2004): A global data set of Palmer Drought Severity Index for 1870-2002: Relationship with soil moisture and effects of surface warming. *J. Hydrometeorology* 5: 1117-1130.

Elfatih, A., Eltahir, B., and Yeh, P.J.F., (1999): On the asymmetric response of aquifer water level to floods and droughts in Illinois, *Water Resources Research* 35: 1199–1217.

Heim, R.R., (2002): A review of twentieth-century drought indices used in the United States. *Bulletin of the American Meteorological Society.* 83: 1149-1165.

Hoffman, M.T., Carrick, P.J., Gillson, L. and West, A.G. (2009): Drought, climate change and vegetation response in the succulent karoo, South Africa. *South African Journal of Science* 105: 54-60.

Hosking, J.R.M., (1990): L-Moments: Analysis and estimation of distributions using linear combinations of order statistics. *Journal of Royal Statistical Society B,* 52: 105-124.

Ji, L. and Peters, A.J., (2003): Assessing vegetation response to drought in the northern Great Plains using vegetation and drought indices. *Remote Sensing of Environment.* 87: 85-98.

Karl, T.R., (1983): Some spatial characteristics of drought duration in the United States. *Journal of Climate and Applied Meteorology* 22: 1356-1366.

Karl, T.R., (1986): The sensitivity of the Palmer Drought Severity Index and the Palmer z-Index to their calibration coefficients including potential evapotranspiration. *Journal of Climate and Applied Meteorology,* 25: 77-86.

Keyantash, J. and Dracup., J., (2002): The quantification of drought: an evaluation of drought indices. *Bulletin of the American Meteorological Society*. 83: 1167-1180.

Khan, S., Gabriel, H.F. and Rana, T. (2008): Standard precipitation index to track drought and assess impact of rainfall on watertables in irrigation areas. *Irrigation and Drainage Systems* 22: 159-177.

López-Moreno, J.I., Vicente-Serrano, S.M., Beguería, S. García-Ruiz, J.M., Portela, M. M., Almeida, A. B. (2009): Downstream propagation of hydrological droughts in highly regulated transboundary rivers: the case of the Tagus River between Spain and Portugal. *Water Resources Research* 45, W02405, doi:10.1029/2008WR007198.

Lorenzo-Lacruz, J., Vicente-Serrano, S.M., López-Moreno, J.I., Beguería, S., García-Ruiz, J.M. and Cuadrat, J.M. (2010) The impact of droughts and water management on various hydrological systems in the headwaters of the Tagus River (central Spain). *Journal of Hydrology*. In press.

McKee, T.B.N., Doesken, J. and Kleist, J., (1993): The relationship of drought frequency and duration to time scales. *Eighth Conf. On Applied Climatology*. Anaheim, CA, Amer. Meteor. Soc. 179-184.

Mitchell, T.D. and Jones, P.D. (2005): An improved method of constructing a database of monthly climate observations and associated high-resolution grids. *International Journal of Climatology* 25: 693-712.

Palmer, W.C., (1965): *Meteorological droughts.* U.S. Department of Commerce Weather Bureau Research Paper 45, 58 pp.

Pandey, R. P. and Ramasastri, K. S., (2001): Relationship between the common climatic parameters and average drought frequency. *Hydrological Processes* 15: 1019–1032, 2001.

Patel, N.R., Chopra, P., and Dadhwal, V.K. (2007): Analyzing spatial patterns of meteorological drought using standardized precipitation index. *Meteorological Applications*, 14: 329-336.

Sternberg, T., Middleton, N. and Thomas, D. (2009): Pressurised pastoralism in South Gobi, Mongolia: What is the role of drought?. *Transactions of the Institute of British Geographers* 34: 364-377.

Szalai, S., Szinell, C.S. and Zoboki, J., (2000): Drought monitoring in Hungary. In *Early warning systems for drought preparedness and drought management.* World Meteorological Organization. Lisbon: 182-199.

Thornthwaite, C.W., (1948): An approach toward a rational classification of climate. *Geographical Review.* 38: 55-94.

van der Schrier, G., Briffa, K.R., Jones, P.D. and Osborn, T.J., (2006a): Summer moisture variability across Europe. *Journal of Climate* 19: 2818-2834

van der Schrier, G., Briffa, K.R., Osborn, T.J. and Cook, E.R., (2006b): Summer moisture availability across North America. *Journal of Geophysical Research* 111, D11102 (doi:10.1029/2005JD006745).

Vicente Serrano, S.M. and López-Moreno, J.I., (2005): Hydrological response to different time scales of climatological drought: an evaluation of the standardized precipitation index in a mountainous Mediterranean basin. *Hydrology and Earth System Sciences* 9: 523-533.

Vicente-Serrano, S.M. (2007): Evaluating the impact of drought using remote sensing in a Mediterranean, semi-arid region, *Natural Hazards* 40: 173-208.

Vicente-Serrano S.M., Santiago Beguería, Juan I. López-Moreno, (2010): A Multi-scalar drought index sensitive to global warming: The Standardized Precipitation Evapotranspiration Index – SPEI. *Journal of Climate* 23: 1696–1718.

Wells, N., Goddard, S. and Hayes, M.J., (2004): A self-calibrating Palmer Drought Severity Index. *Journal of Climate* 17: 2335-2351.

Figure legends

Figure 1. Spatial distribution of P-values obtained from the Kolmogorov-Smirnov test used to determine the goodness of fit between the global monthly series of D and the log-logistic distribution.

Figure 2. Spatial distribution of the UCAR PDSI and the SPEI (3, 9, 12, 24, and 36 months) for the European continent, August 1936.

Figure 3. Spatial distribution of the CRU sc-PDSI and the SPEI (3, 6, 9, 12, 18, 24 and 36 months) for the European continent, November 1949.

Figure 4: Average and standard deviation values of correlation (R-Pearson) between the time series of the sc-PDSI for Europe and North America, and various time scales of the SPEI and the global PDSI.

Figure 5: Spatial distribution of the correlation between the time series of UCAR PDSI and the SPEI at different time scales. The time scale in which the maximum correlation was recorded is indicated in the lower plate.

Figure 6: Spatial distribution of the correlation between the time series of CRU sc-PDSI and the SPEI at different time scales in Europe. The time scale in which the maximum correlation was recorded is indicated in the lower plate.

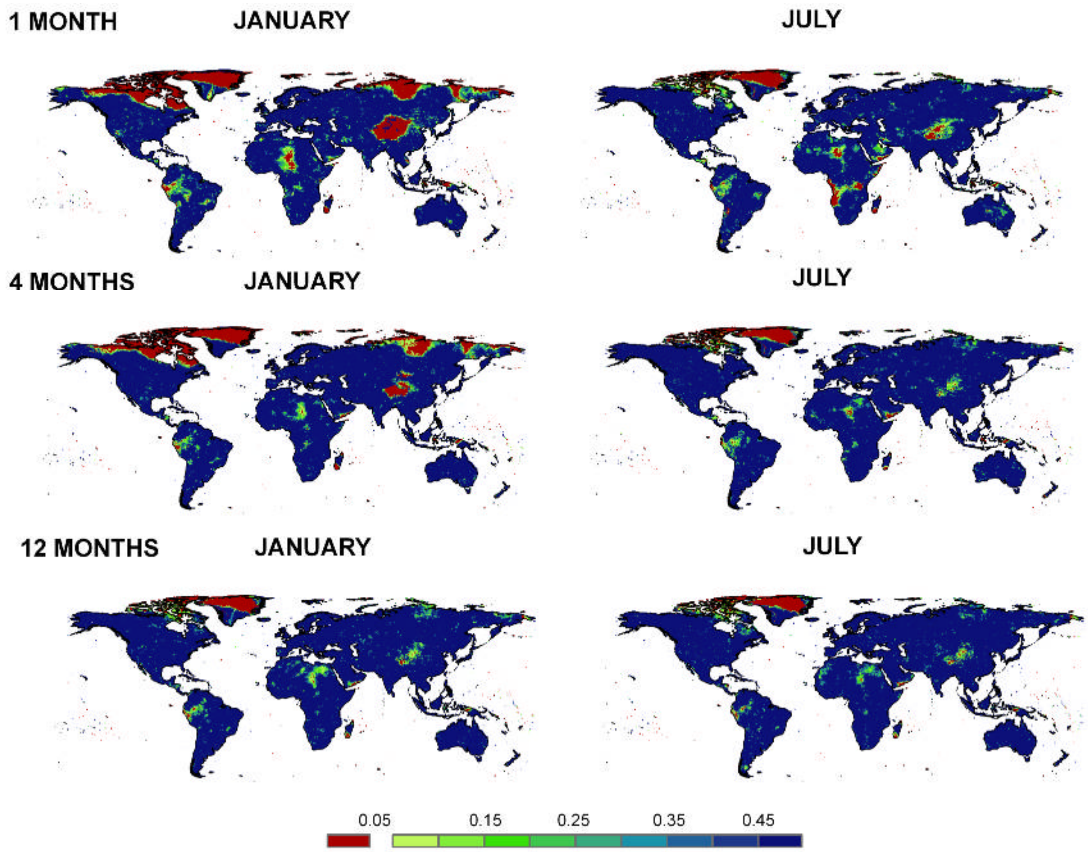

Figure 1. Spatial distribution of P-values obtained from the Kolmogorov-Smirnov test used to determine the goodness of fit between the global monthly series of D and the log-logistic distribution.

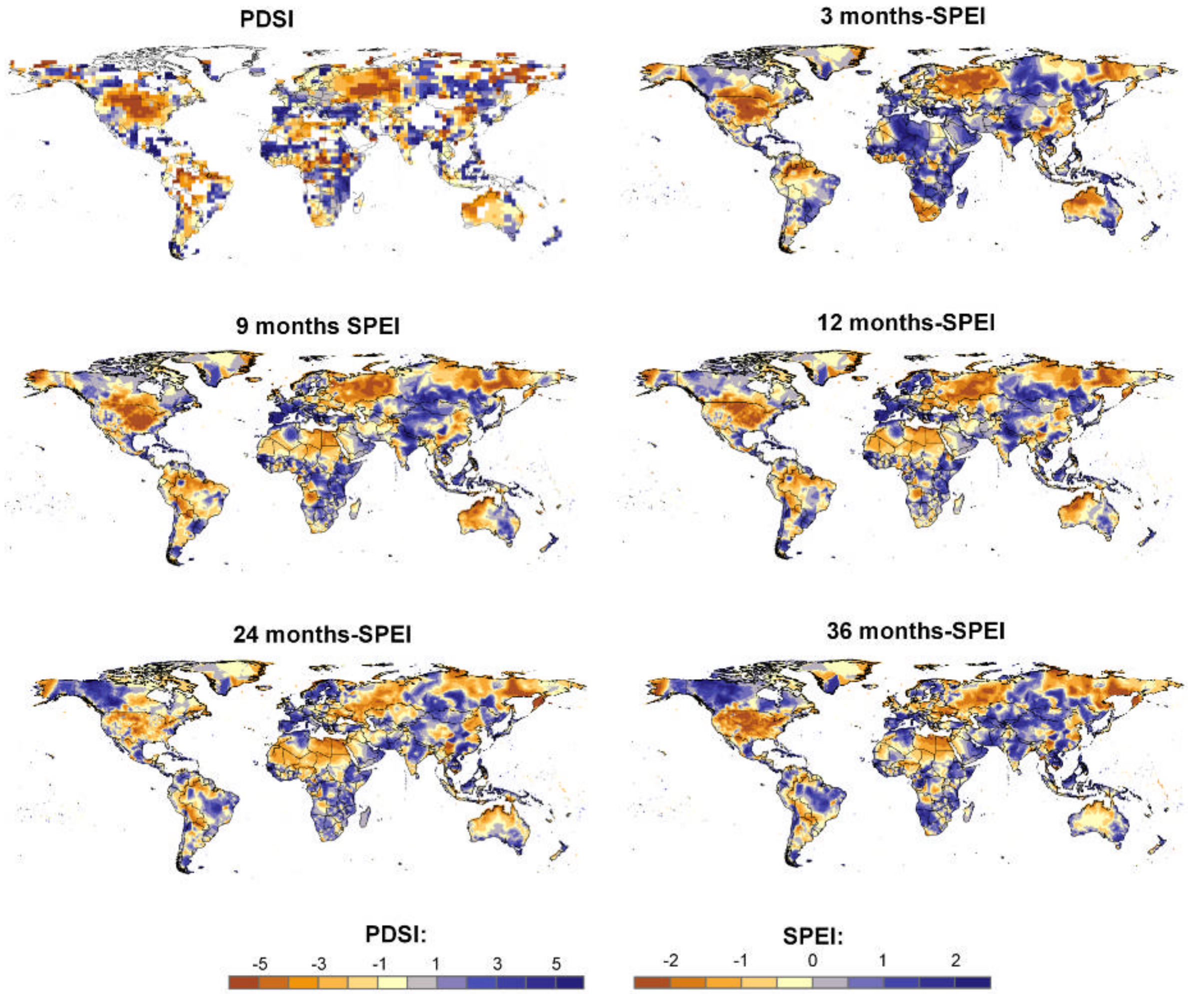

Figure 2. Spatial distribution of the global UCAR PDSI and the SPEI (3, 9, 12, 24, and 36 months), August 1936.

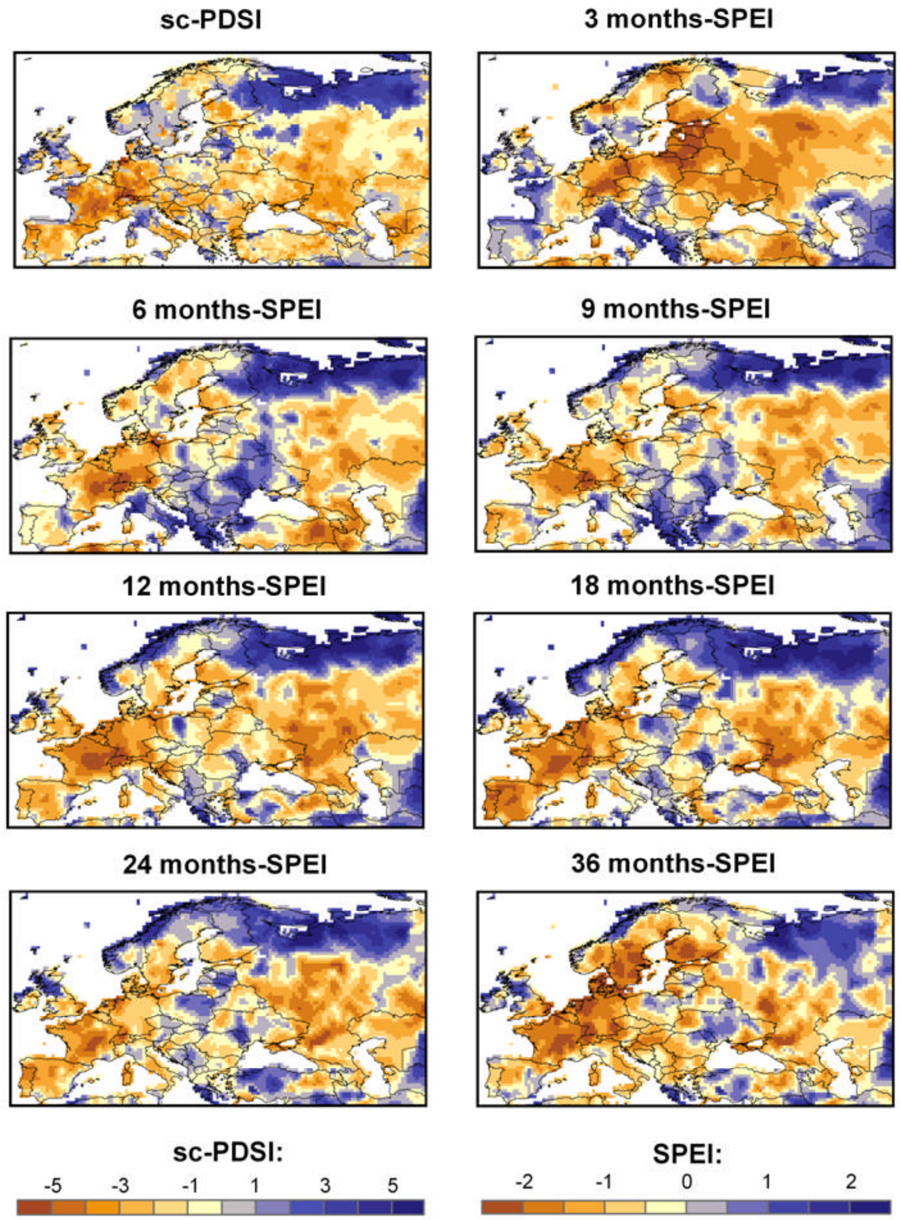

Figure 3. Spatial distribution of the CRU sc-PDSI and the SPEI (3, 6, 9, 12, 18, 24 and 36 months) for the European continent, November 1949.

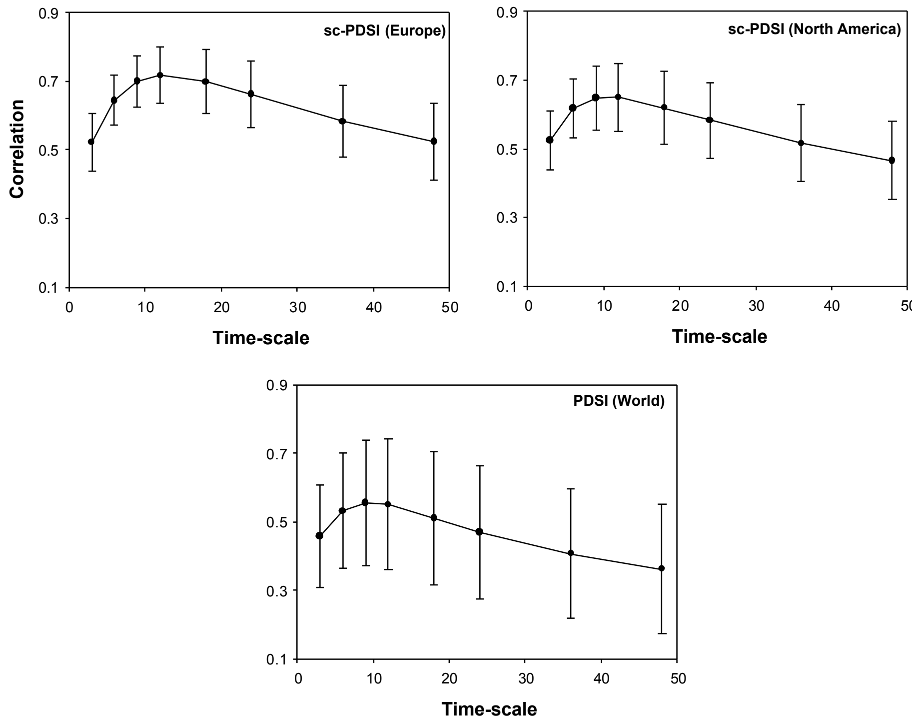

Figure 4: Average and standard deviation values of correlation (*R*-Pearson) between the time series of the sc-PDSI for Europe and North America, and various time scales of the SPEI and the global PDSI.

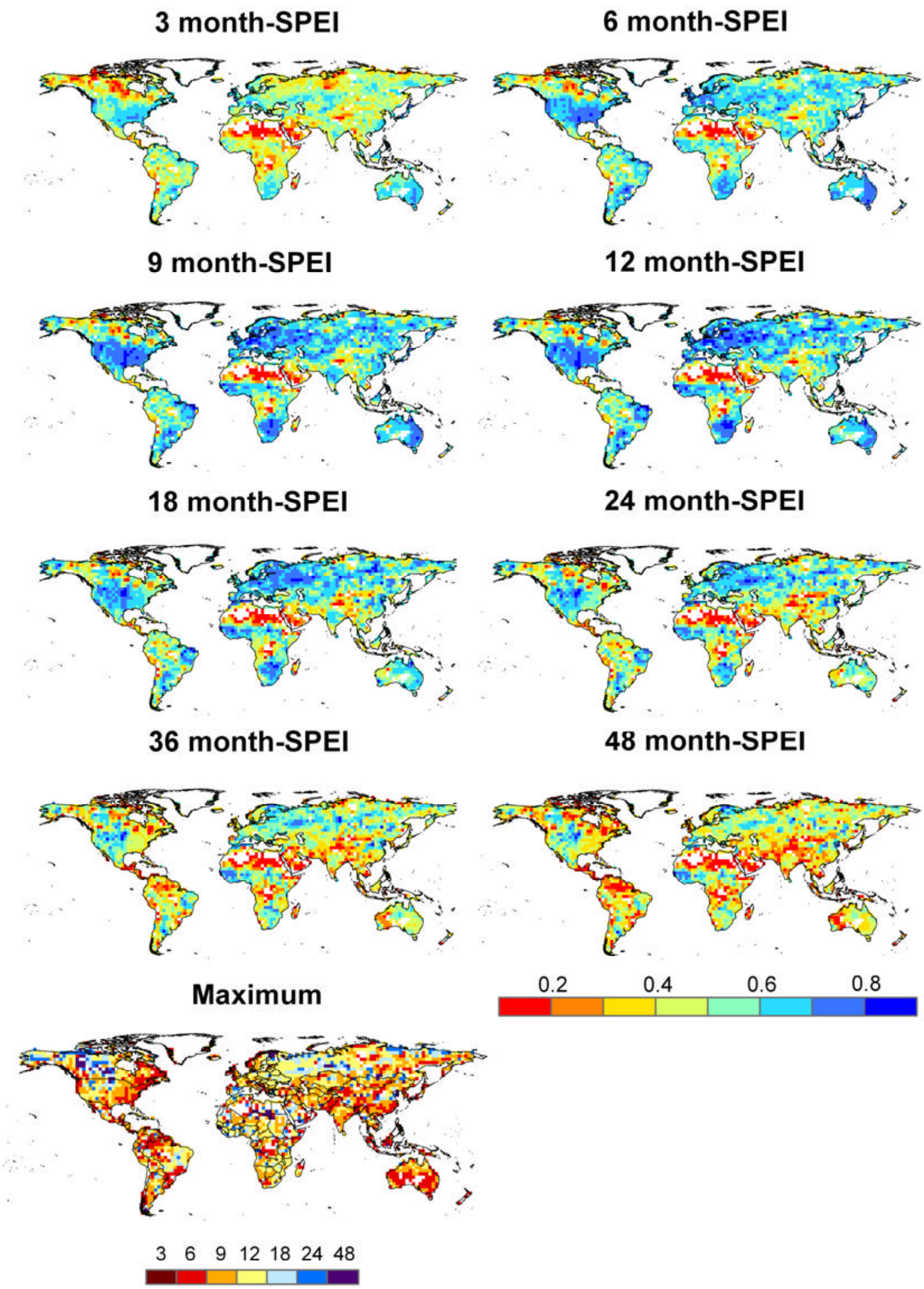

Figure 5: Spatial distribution of the correlation between the time series of UCAR PDSI and the SPEI at different time scales. The time scale in which the maximum correlation was recorded is indicated in the lower plate.

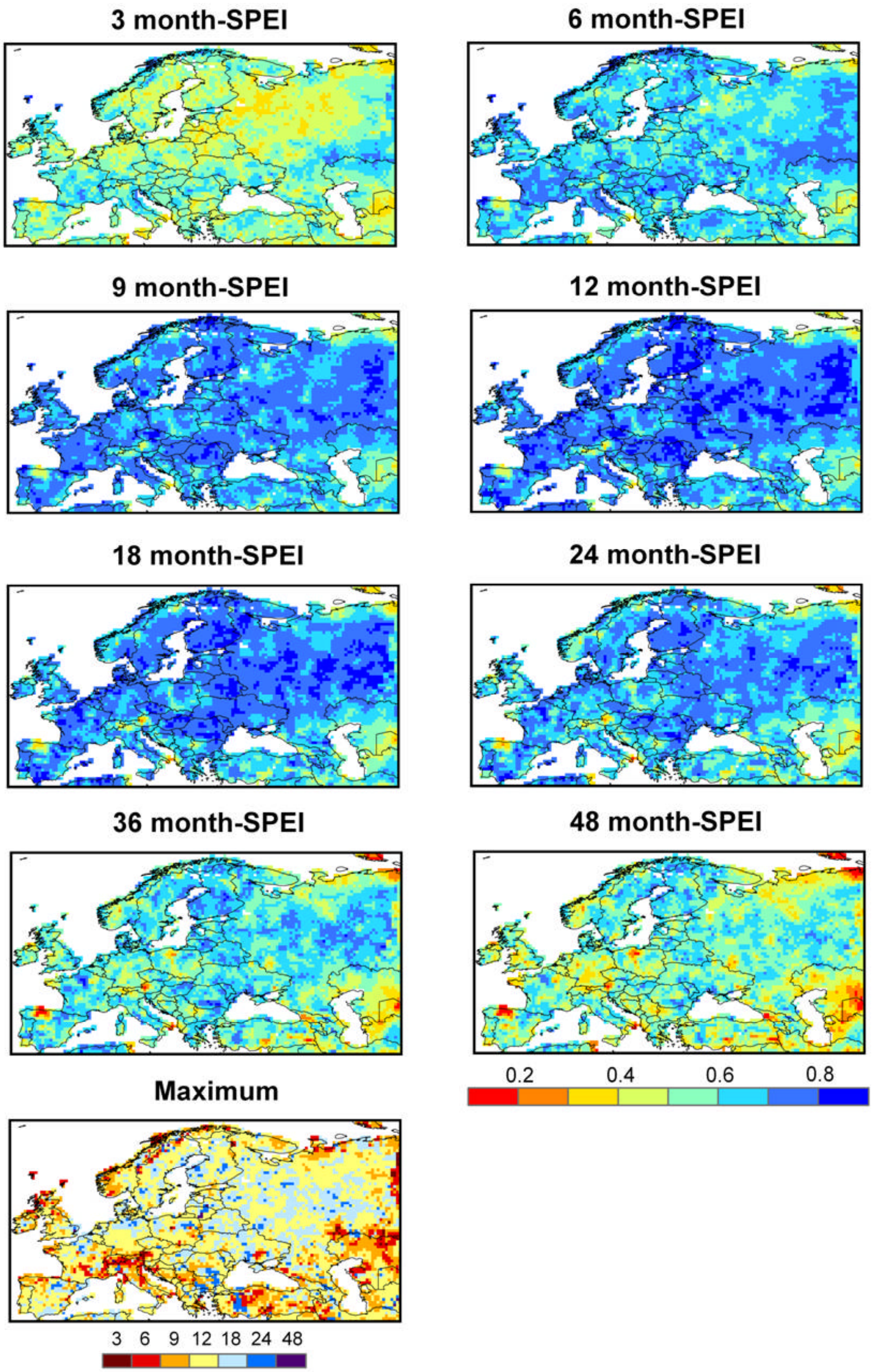

Figure 6: Spatial distribution of the correlation between the time series of CRU sc-PDSI and the SPEI at different time scales in Europe. The time scale in which the maximum correlation was recorded is indicated in the lower plate.